Original Article

Sensitivity of GAGG based scintillation neutron detector with SiPM readout

A. Fedorov [a, b], V. Gurinovich [c], V. Guzov [c], G. Dosovitskiy [b], M. Korzhik [a, b, *],
V. Kozhemyakin [c], A. Lopatik [c], D. Kozlov [a], V. Mechinsky [a], V. Retivov [b]

[a] *Institute for Nuclear Problems of Belarus State University, Minsk, Belarus*
[b] *NRC Kurchatov Institute, Moscow, Russia*
[c] *ATOMTEX SPE, Minsk, Belarus*

ARTICLE INFO

ABSTRACT

Here we report on the first results of sensitivity evaluation of the gadolinium-aluminum-gallium- garnet (GAGG) scintillation detector with SiPM readout to fast and slow neutrons and, to the natural background and Co-60 γ-radiation as well. Data on sensitivity were obtained using certified dosimetry benches, so it can be utilized in the calculation of detection limits of neutron flux with such type of detectors. It was concluded that use of GAGG scintillator has a good prospect for neutron monitoring in different parts of nuclear research reactors and power plants.

1. Introduction

The multicomponent garnet-type scintillators, in particular, $Gd_3Al_2Ga_3O_{12}$ doped with Ce (GAGG) single crystal, show spectacular progress in the improvement of their scintillation properties [1–3]. They exhibit an attractive combination of a high light yield of up to 58,000 ph/MeV, a short luminescence decay time of less than 100 ns [4–6] and good, compared to a PMT, matching of the emission spectrum peaked at 520 nm with the sensitivity spectra of SiPMs. The timing properties of GAGG:Ce scintillator might be substantially improved by co-doping the crystal with magnesium [7,8].

Recently, it was shown that GAGG:Ce scintillator and its modification, multi-doped GAGG:Ce, Mg, Ti [9] are suitable for neutron detection [10,11]. GAGG was found to be superior to Gd_2SiO_5:Ce [12,13] and GdI_3:Ce [14] scintillation crystals due to a better light yield, mechanical and chemical stability and tolerance to irradiation with ionizing radiation, particularly with hadrons [15].

Due to the fact that gadolinium natural isotopic composition has

the thermal neutron's absorption cross-section of 49,000 b and an extended region of resonances in the energy range from 1 eV to 10 keV, Gd containing scintillators are capable to detect neutrons in an expanded energy. Moreover, at higher neutron energy, the other reaction channels such as inelastic scattering become open, increasing the stopping power of the material to neutrons. As a result, in addition to thermal neutrons, gadolinium containing scintillation material could be assumed to be an efficient detector of epithermal and fast neutrons. This makes a high light yield GAGG based scintillation detector a prospective solution for the detection of neutrons in different points of research reactors and nuclear power plants as well.

For gadolinium, the main reaction channel for slow neutrons is neutron radiative capture (n,γ), at which excited composite gadolinium nucleus emits multiple γ-quanta with a total energy of about 8 MeV [16]. At transitions to the ground state from lowest excited energy levels of the nuclei of gadolinium isotopes the soft γ-quanta can be emitted along with x-rays [17] and internal conversion electrons [12,13]. Due to this reason, an efficient gadolinium-based neutron detector should be an effective detector of γ-quanta possessing good energy resolution through the highest available light yield of the scintillation material. This is the main inherent drawback of any gadolinium-based neutron detector — increased sensitivity to gamma radiation, e.g. natural radioactive background, especially in comparison with He-3 neutron counters.

---

* Corresponding author. Institute for Nuclear Problems of Belarus State University, Minsk, Belarus.

E-mail address: mikhail.korjik@cern.ch (M. Korzhik).

In our study, we elaborated a concept to the creation of the combined neutron-gamma handheld spectrometric appliance, with working energy range from 30 to 1000 keV in neutron detection mode and from 30 to 3000 keV in γ-quanta detection mode. In neutron detection mode, lead background shielding surrounds GAGG crystal from all sides, with optional polyethylene moderator attached over lead shielding. In a γ-quanta detection mode, the front part of the lead shielding can be removed.

2. Experimental

Detector was based on GAGG scintillation crystal with dimensions $14 \times 14 \times 10$ mm^3, wrapped in TEFLON light reflector and coupled with an optical grease to a 2×2 SiPM array SensL ARRAYJ-60035-4P-BGA [18]. The light yield of the GAGG crystal was 40,000 ph/MeV, its output area read out by SiPMs was 196 mm^2, total sensitive area of four SiPMs - 144 mm^2. SiPM 2×2 array was mounted on a small PCB equipped with temperature sensor. Crystal and PCB were fixed inside thin (~2 mm) plastic case and put into 15 mm Pb/3 mm Cu shielding of 4π geometry, providing a suppression in the background count rate by factor 22 in the energy range from 50 to 150 keV. SiPM and temperature sensor bias and signals are delivered with 10 mm wide and 50 mm long flexible flat cable through 12×2 mm sloped groove inside the shielding as it is shown in Fig. 1.

The SiPMs had common bias, but their signals were merged into two pairs. A flexible flat cable connected SiPMs and temperature sensor with another PCB, containing: DC-DC convertors including bias one adjusted by temperature sensor signal; spectrometric amplifier with 600 ns shaping time constant and coincidence circuit to suppress high temperature SiPM noise (actually used only in high temperature evaluations). Detector was powered from a USB socket, current consumption from 5 V power supply was 6—8 mA. Detector outer aluminum case had dimensions of Ø 60 × 200 mm and weight with shielding was 1.5 kg.

We used two facilities and two acquisition systems in present research. First one was a laboratory with Peltier cooled/heated thermal camera and acquisition based on ORTEC MCA PC board with lower and upper level discriminators (LLD, ULD) adjustable in acquisition software. Here we also studied the energy scale linearity. During all these measurements Pb/Cu shielding was removed.

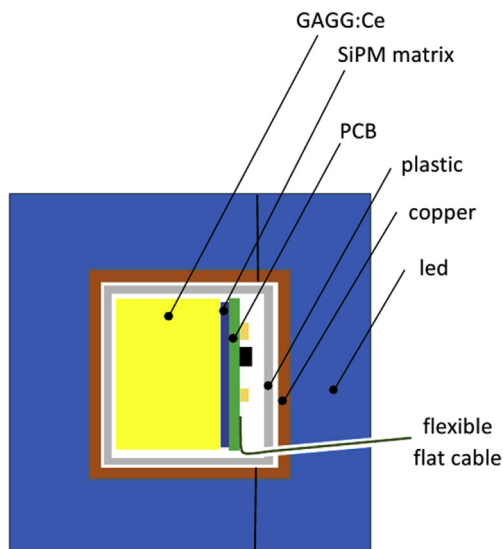Second one was irradiation facility with neutron and gamma-dosimetry benches, where acquisition was based on another, portable MCA, with spectroscopy grade integral and differential linearity, but with LLD set at 45 keV by hardware, without possibility to adjust. Instead, this MCA was the only option available for remote operation from operator room. Calibration with a Cs-137 source was made prior to all measurements.

Fig. 2 shows calibration spectra of γ-sources with energies 59.6 keV (Am-241), 511 keV (Na-22) and 662 keV (Cs-137) measured in laboratory. All spectra were recorded at room temperature using ORTEC TRUMP PCI-2k MCA, with LLD set to 20 keV. Energy resolution at 662 keV was found to be 8.5% FWHM. $14 \times 14 \times 10$ mm^3 GAGG crystal exhibits good photo fractions at 511 and 662 keV. Calculated linearity of the detector energy scale is shown in Fig. 3. Equivalent noise threshold, energy resolution and peak position of Am-241 source 59.6 keV γ-line were evaluated in a thermal camera in the temperature range from $-1.5°$C to $+52.5°$C. Results are presented in Figs. 4—6.

Measurements of the detector sensitivity to fast and slow neutrons were performed at Atomtex (Belarus) irradiation facilities, a 150 m^2 room providing low level of neutron scattering on the construction elements and materials, using the certified neutron dosimetry bench AT140 with ^{238}Pu—Be source (Fig. 7) in accordance to the standard methodic [19]. The bench and acquisition system are controlled from operator room. The ^{238}Pu—Be source moves from the underground protective barrel filled with a neutron absorber to the working position opposite to the detector. In this position, the source is also surrounded with a neutron absorber from all sides, excepting the detector side. Detector was placed at 100 cm distance from the open source in fast neutron mode. Fast neutron flux in measurement point was equal to 235 neutrons/cm^{2}s, which corresponds to an equivalent ambient dose rate H*(10) of 330 mSv/hour. According to the standard methodic, the procedure includes three steps: 1) measurement of the detector response to the direct beam, 2) measurement of the detector response to the scattered neutron fraction with a 40 cm long absorbing cone made of borated paraffin and inserted between the source and detector, and 3) subtraction of this scattered fraction from the detector response in the direct beam. For the Atomtex irradiation facilities, this fraction of the neutrons scattered due to the interaction with walls, constructions, floor and ceiling was found to be equal to 7% ± 1% of total detector response.

The procedure of spectra subtraction also removes a fraction of signal counts, caused by the presence of 4.439 MeV gamma-line from reaction ^{9}Be(α,n)^{12}C* in Pu—Be source to a degree, defined by the 4.439 MeV gamma-quanta absorption in a polyethylene cone. On the other hand, the signal from these gamma-quanta is
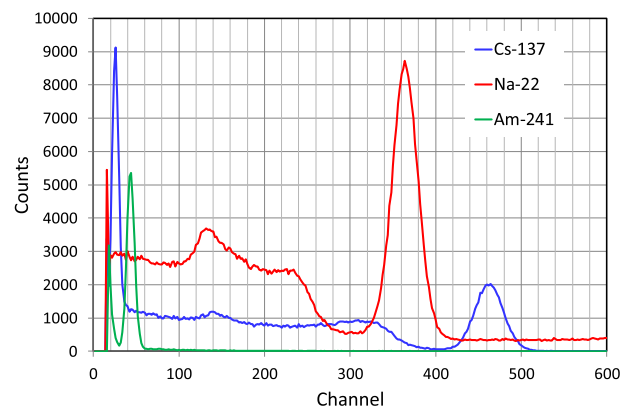

Fig. 1. GAGG detector in the background shielding.

Fig. 2. Recorded calibration spectra of gamma sources with energy 59.6 keV (Am-241), 511 keV (Na-22) and 662 keV (Cs-137). Pb/Cu background shielding is removed.
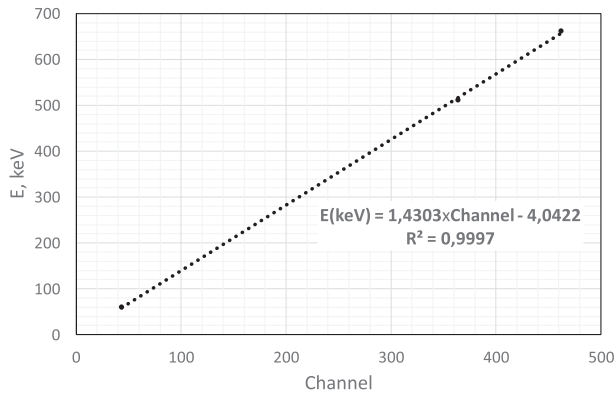
Fig. 3. Linearity of the detector energy scale in range from 59.6 keV to 662 keV.
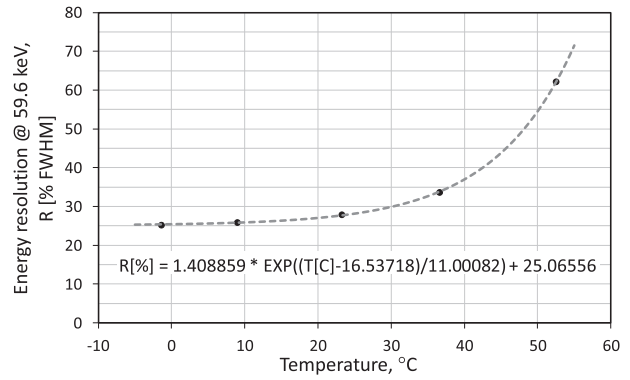

Fig. 6. Energy resolution at 59.6 keV, % FWHM, measured in range from −1.5°C to +52.5°C.
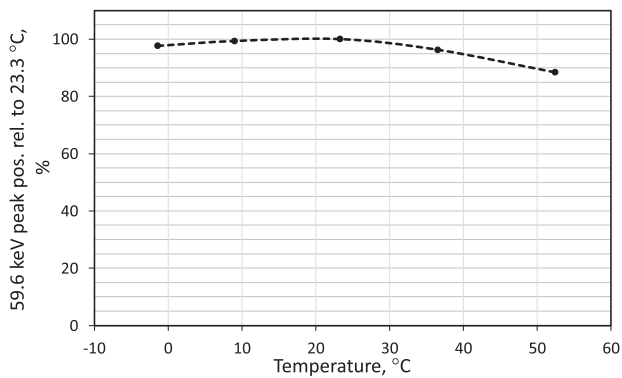

Fig. 4. Temperature stability of the energy scale (temperature dependence of Am-241 peak position) relative to 23.3°C in the range from −1.5°C to +52.5°C. Temperature compensation of SiPM bias +22.6 mV/°C.

Fig. 7. Atomtex neutron irradiation facilities with reference neutron dosimetry bench AT140.
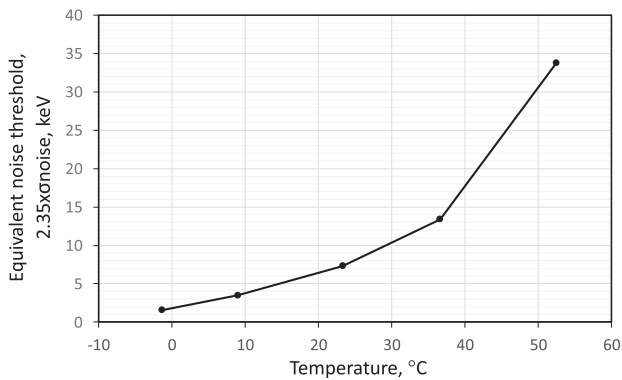
Fig. 5. Equivalent noise threshold, 2.35×σnoise, keV, measured in range from −1.5°C to +52.5°C.
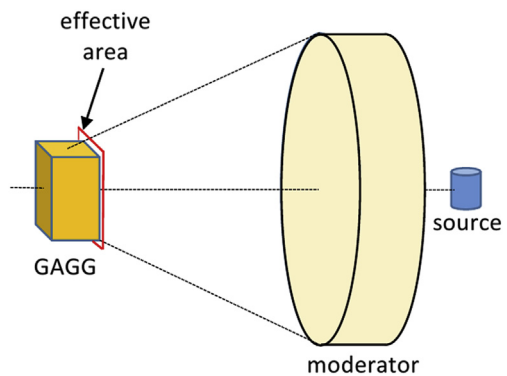

Fig. 8. Effective detector area for slow neutrons.

already suppressed by the detector shielding (nearly 2 times), and sensitivity of 1 cm thick GAGG to such high-energy gamma-quanta is low. Soft gamma-lines present in ^{238}Pu radiation are effectively absorbed in the detector shielding.

We have determined the detector sensitivity as a number of the detector counts per second per unit of neutron flux, measured in $(cm^2 s)^{-1}$. Neutron detection efficiency was determined as the ratio of sensitivity to the effective detector area in cm^2 and expressed in percent. Its meaning is the probability to detect a neutron due to an

interaction into the scintillation crystal. The linear dimensions of the ^{238}Pu–Be source are close to these of the GAGG crystal; so the effective area of the detector in the case of fast neutrons detection was considered to be 1.96 cm^2 — the detector area, visible from the source location.

In a slow neutron mode, the distance between the source and the detector was the same, 100 cm, but 15 cm thick polyethylene moderator block with 30 cm diameter was placed in front of the source. The distance between the moderator front surface and the detector was 80 cm. According to the standard methodic, the procedure for slow neutrons also includes three steps: 4) measurement of the detector response with the moderator installed in front of source, 5) measurement of the detector response with 1 mm Cd filter additionally installed in front of moderator, and 6) subtraction of the second response from the first one. This differential signal corresponds to a flux of slow neutrons in the energy range from 0.0253 eV to 0.4 eV, and its value in the measurement point was equal to 25.0 neutrons/cm^{2}s.

In this case, the procedure of spectra subtraction removes a fraction of signal counts, caused by presence of 4.439 MeV gamma-line virtually completely to a degree, defined by 4.439 MeV gamma-quanta absorption in 1 mm Cd filter.

Here we also determine the detector sensitivity as a number of the detector counts per second per unit neutron flux in (cm^{2}s)$^{-1}$. Since moderator dimensions far exceed that of GAGG crystal, the effective area of the detector for slow 0.0253 eV–0.4 eV neutrons was determines as 2.54 cm^2 ± 7% – the effective detector area, visible from the moderator location and used in the efficiency calculations, as shown in Fig. 8.

All fluxes and dose rate errors of AT140 bench with ^{238}Pu–Be source were protocolled at Nov. 6, 2018 to be within ±4%, with 95% probability (statistical confidence interval). Correction on 87.7 years ^{238}Pu half-decay was applied on the measurement date. Detector positioning error did not exceed ±1 cm relative to the source in all measurements.

According to Ref. [20], neutron dosimeters and radiometers should undergo testing of their sensitivity to gamma-radiation background, produced by Cs-137 or Co-60 sources. Measurements

of the neutron detector sensitivity to gamma-radiation from Co-60 were also performed at Atomtex irradiation facilities using certified Co-60 dosimetry bench. Co-60 source moves from the protective underground shield to the working position opposite to the detector, in which the detector was placed at 100 cm distance from the open Co-60 source, with positioning error ±1 cm. At 100 cm distance, the ambient dose rate of gamma-radiation from Co-60 amounted to 9.8 μSv/hour, with dose rate error ±5%. Measurements of the neutron detector sensitivity to natural γ-radiation background were performed at the same facility when the Co-60 source was in "safe" position in the shield. The ambient dose rate of the γ-radiation background amounted to 0.1 μSv/hour in this position.

All measurements under neutrons and Co-60 gammas were performed with Pb/Cu background shielding surrounding GAGG crystal. At neutron measurements, natural background spectrum was subtracted from spectra obtained at steps 1, 2, 4 and 5 prior to steps 3 and 6.

In measurements at Atomtex facilities, we used a USB-powered 1 k MCA with a Wilkinson spectrometric ADC from Atomtex spectrometric detection unit BDKG-201M. LLD setting was 45 keV, upper limit of the linear energy scale was 1000 keV. All events with energy deposit >1000 keV were compressed in a saturation peak on the output of the detector, which area was also used in our sensitivity calculations. This area is equal to the number of signal and background events with energy deposit from 1 MeV to maximum possible energy deposit from high-energy gamma-quanta and charged cosmic particles, tentatively ≥10 MeV. All spectra were acquired in a tablet PC remotely from operator room.

3. Results

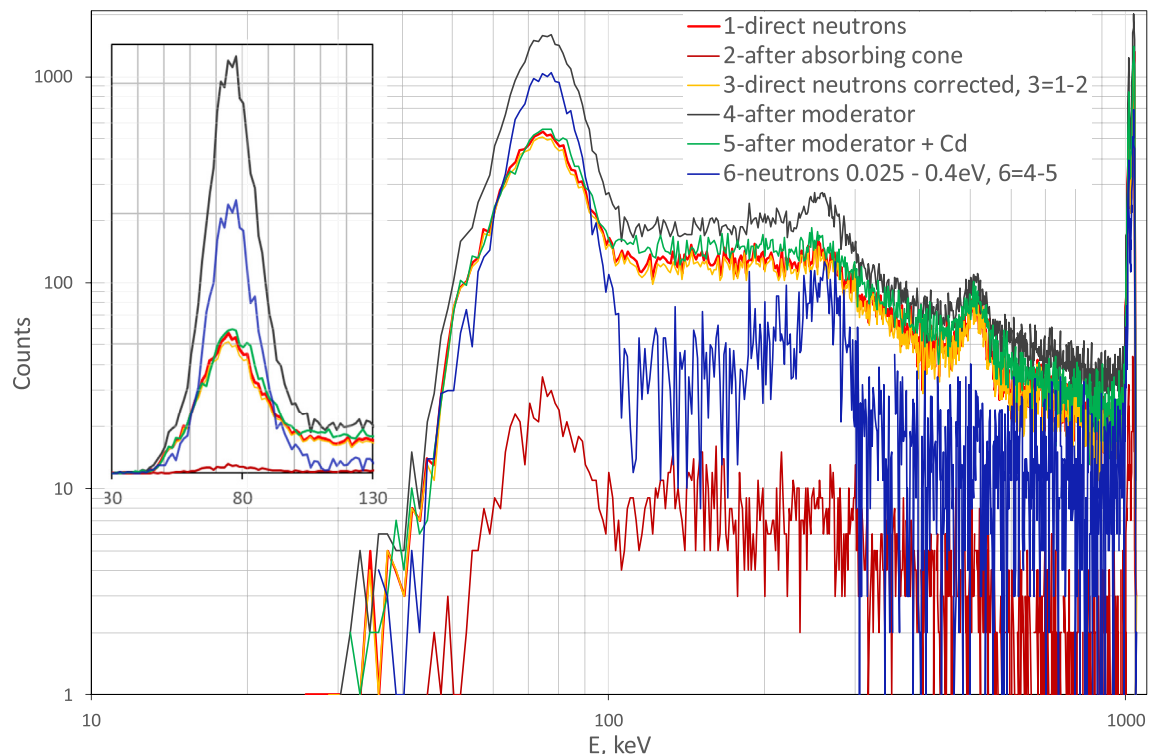Fig. 9 shows the pulse height spectra acquired at neutron

Fig. 9. Pulse height spectra acquired at neutron dosimetry bench AT140 with ^{238}Pu–Be source.
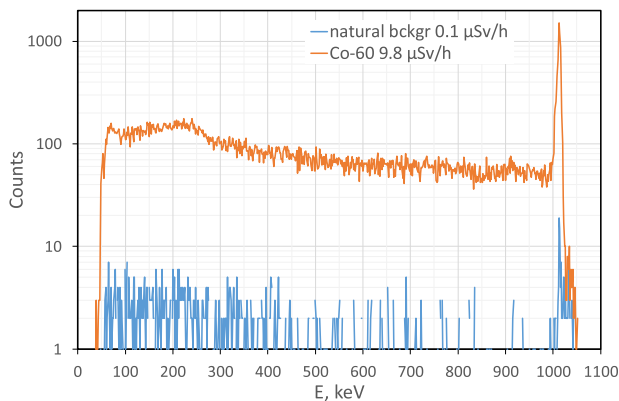
Fig. 10. Pulse height spectra acquired at gamma dosimetry bench with Co-60 source.

dosimetry bench AT140 with ^{238}Pu-be source IBN-9-6 #010. Spectrum 1 was recorded in a direct beam of fast neutrons, with no material between the source and the detector. Spectrum 2 was recorded with the absorbing cone installed in front of the ^{238}Pu−Be source. Spectrum 3 was obtained by subtraction of spectrum 2 from spectrum 1 and represents spectrum of neutrons with flux of 235.0 neutrons/cm^{2}s in the measurement point. Spectrum 4 was recorded with the moderator installed in front of the ^{238}Pu−Be source. Spectrum 5 was recorded with moderator and 1 mm Cd filter both installed in front of the ^{238}Pu-be source. Spectra 1, 2, 4 and 5 are presented in Fig. 9 after subtraction of the spectrum of the natural background presented in Fig. 10 below (measured in the next room with Co-60 bench, with ambient dose rate of 0.1 μSv/hour). All spectra acquisition times were 600 s (live time) including the natural background spectrum. Spectrum 6 was obtained by subtraction of spectrum 5 from spectrum 4 and represents spectrum of neutrons in the energy range from 0.0253 to 0.4 eV with flux of 25.0 neutrons/cm^{2}s in the measurement point.

The increase in count rate from spectrum 1 to 4 is caused by the presence of slow neutrons with high capture cross section. There is also a slight increase in counts even from spectrum 1 to spectrum 5

(after moderator and Cd) − slow neutrons are cut with Cd, however spectrum of fast neutrons is still greatly softened by the moderator above 0.4 eV.

The most prominent line in the spectra has a maximum at 77 keV and, most likely, is a sum of soft γ − lines from transitions to Gd ground states and Gd x-rays coincided with internal conversion (IC) electrons. It also overlaps with the γ-lines with mean energy ~90 keV, observed in our GEANT 4 simulations with fast neutrons [10]. The other detected lines and groups of lines are centered at 511 keV, 250−260 keV, and 190−220 keV.

Calculated values for sensitivity and detection efficiencies for various energy ranges of gamma-quanta starting from 45 keV are listed in Table 1. Sensitivities were calculated from the number of counts within the energy range, known fluxes and acquisition time as explained above. For the moderated neutrons, the neutron detection efficiency is marked as "non-available" (na) due to the difficulty to estimate correctly the effective area of the detector for a mixture of fast and slow neutrons.

Fig. 10 represents the pulse height spectra acquired at gamma dosimetry bench with Co-60 source having the ambient dose rate of 9.8 μSv/hour in the detector point. Natural background with ambient dose rate of 0.1 μSv/hour was measured when Co-60 source was in moved in an underground protective shield. Both spectra acquisition live times were 600 s.

Table 2 summarizes neutron equivalents of count rates from natural background 0.1 μSv/hour and Co-60 1 μSv/hour ambient dose rates, calculated on the base of sensitivities presented in Table 1 and spectra shown in Fig. 10.

4. Discussion

The overall error for sensitivity and efficiency results for the fast neutrons from ^{238}Pu−Be source were estimated to be not exceeding ±5%. The sources of this error are flux and detector positioning errors.

For slow neutrons, the overall error for sensitivity is the same, ±5%. Error or the detection efficiency includes uncertainty of the effective area and would not exceed ±8%, i.e. detection efficiency is in between 91.3% and 100%.

Table 1
Calculated sensitivities and detection efficiencies for various energy ranges of gamma-quanta.

Energy range of gamma-quanta, keV	Direct fast neutrons		Neutrons after moderator		Slow neutrons	
	Sensitivity (neutron/cm^{2}s)	Neutron detection efficiency (%)	Sensitivity (neutron/cm^{2}s)	Neutron detection efficiency (%)	Sensitivity (neutron/cm^{2}s)	Neutron detection efficiency (%)
45−105	0.073	3.74	0.181	na	1.14	44.9
45−305	0.182	9.29	0.365	na	1.64	64.6
45−550	0.247	12.6	0.464	na	1.80	71.0
45−1000	0.298	15.2	0.554	na	2.04	80.3
45->10,000	0.384	19.6	0.714	na	2.52	91.3

Table 2
Neutron equivalents of count rates from natural background 0.1 μSv/hour and Co-60 1 μSv/hour.

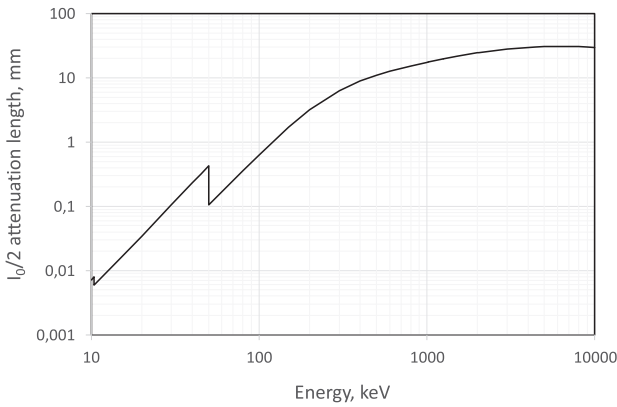| Energy range of gamma-quanta (keV)	Fast neutrons		Neutrons after moderator		Slow neutrons	
	Neutron equivalent of count rate from natural background 0.1 μSv/hour (n/cm^{2}s)	Neutron equivalent of count rate from Co-60 1.0 μSv/hour (n/cm^{2}s)	Neutron equivalent of count rate from natural background 0.1 μSv/hour (n/cm^{2}s)	Neutron equivalent of count rate from Co-60 1.0 μSv/hour (n/cm^{2}s)	Neutron equivalent of count rate from natural background 0.1 μSv/hour (n/cm^{2}s)	Neutron equivalent of count rate from Co-60 1.0 μSv/hour (n/cm^{2}s)
45−105	2.07	10.6	0.837	4.28	0.133	0.679
45−305	3.85	21.6	1.92	10.8	0.428	2.39
45−550	4.40	25.2	2.34	13.4	0.603	3.45
45−1000	4.86	31.1	2.61	16.7	0.709	4.55
45->10,000	4.27	27.6	2.30	14.9	0.649	4.19

Fig. 11. Attenuation length of GAGG for gamma radiation due to photo effect, Compton scattering and pair production.

In fact, the slow 0.0253 eV–0.4 eV neutrons are completely absorbed in a $14 \times 14 \times 10$ mm^3 GAGG crystal according to GEANT 4 simulations however, one can suppose some fraction of not coincidently summed events with the energy deposition below 45 keV in the recorded spectra, for example, Gd characteristic radiation [11] (Gd Kα1 = 43 keV), but we have no indications on its shoulder in our spectra. Moreover, due to internal conversion coefficients $\alpha\kappa = 2.4$, mostly the events of x-ray leakage, producing a 33 keV IC-electron peak [9,13]. The 80–90 keV gamma-quantum from the same nuclei transitions to the ground state has the same probability to escape from the surface area of GAGG without interaction as a 43 keV x-ray, Fig. 11, calculated using [21]. Finally, one can expect, that some events of neutron capture could happen without emission of at least one electron, x-ray or γ-quantum soft enough to be effectively absorbed in a $14 \times 14 \times 10$ mm^3 GAGG crystal. On the other hand, values of the detection efficiency obtained by us give evidence that the fraction of all such events would not exceed 8% in

this detector as already mentioned above.

Unfortunately, this 8% efficiency loss seems to be practically unavoidable in a portable SiPM based device. The studied SiPM/GAGG based detector cannot perfectly operate at higher than laboratory temperatures in a mode without coincidences between SiPMs and gated ADC. Normally, for measurement of low radionuclide activities or particle fluxes LLD should be set noticeably above the value of the equivalent noise threshold at the highest working temperature. Operation at T = 50 °C with LLD set to 30 keV is only possible in coincidence mode, otherwise, it must be set at ~100 keV at least, Fig. 12. However, even coincidence mode will not eliminate dead time increase and energy resolution degradation.

The overall error for the neutron equivalents of count rates from natural background 0.1 μSv/hour did not exceed ±22% for 45–105 keV energy range and ±12% for all others - sum inaccuracy of a reference dosimeter and poorness of statistics in the acquired spectrum. The overall error for neutron equivalents of count rates from Co-60 did not exceed ±8%, which represents the root mean square error of the combined dose rate, statistical and positioning uncertainties.

The described detector demonstrates high sensitivity to the fast neutrons. Use of a moderator would further improve it. At the same time, the neutron equivalents of count rates from Co-60 and even from the natural background might seem to be high. Of course, for a specialized thermal neutron detector 10 mm thickness is excessive, it can be significantly reduced without critical loss of sensitivity to neutrons, but with a significant gain in neutron/gamma sensitivity ratio. However, for a concept of combined neutron-gamma spectrometric appliance gamma sensitivity is important too. On the other hand, 260 keV and especially 77 keV groups of lines are very prominent and easily extracted in spectra processing. Other feasible ways to eliminate the unwanted influence of gamma-background are more lead shielding and/or an additional gamma-detector, which is not sensitive to neutrons for differential measurements.
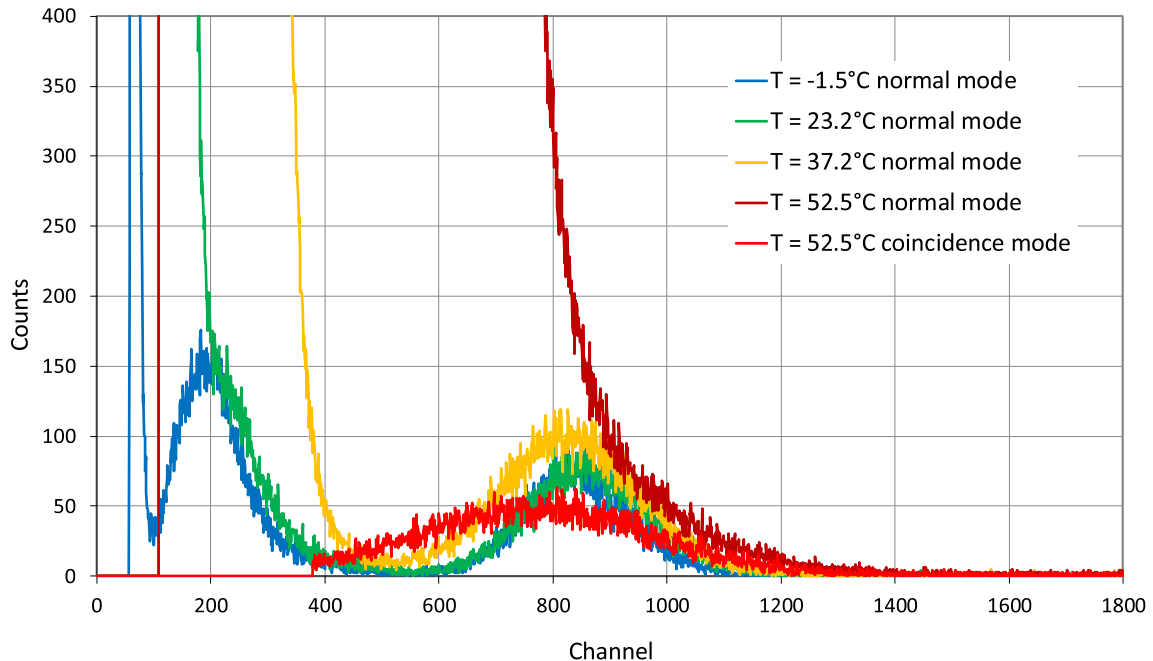

Fig. 12. Pulse height spectra of ~300 Bq Am-241 source acquired at different temperatures in "normal" and "SiPM coincidence" modes in 300 s.

5. Conclusion

The data on the $14 \times 14 \times 10$ mm^3 GAGG scintillation crystal sensitivity and detection efficiency to fast and slow neutrons and to γ-radiation were obtained using a high-performance detector prototype based on a SiPM matrix. As far as the sensitivity values were obtained at facilities equipped with the certified dosimetry benches, the data can be used to estimate capabilities and the GAGG/SiPM detector limitations for the fluxes of fast and slow neutron under different background conditions at the reactors.

Declaration of competing interest

The authors declare that they have no known competing financial interests or personal relationships that could have appeared to influence the work reported in this paper.

Acknowledgement

References

[1] P. Lecoq, A. Gektin, M. Korzhik, Inorganic Scintillators for Detecting Systems, Springer, 2017.
[2] Kamada, et al., Composition engineering in cerium-doped (Lu,Gd)3(Ga,Al)5O12 single-crystal scintillators, Cryst. Growth Des. 11 (2011) 4484–4490.
[3] Kamada, et al., 2inch diameter single crystal growth and scintillation properties of Ce:Gd3Al2Ga3O12, J. Cryst. Growth 352 (2012) 88–90.
[4] K. Kamada, M. Nikl, S. Kurosawa, A. Beitlerova, A. Nagura, Y. Shoji, J. Pejchal, Y. Ohashi, Y. Yokota, A. Yoshikawa, Alkali earth co-doping effects on luminescence and scintillation properties of Ce doped Gd3Al2Ga3O12 scintillator, Opt. Mater. 41 (2015) 63–66.
[5] Kamada, et al., Cz grown 2-in. size Ce:Gd3(Al,Ga)5)12 single crystal; relationship between Al,Ga site occupancy and scintillation properties, Opt. Mater. 36 (2014) 1942–1945.
[6] M. Korjik, V. Alenkov, A. Borisevich, O. Buzanov, V. Dormenev, G. Dosovitskiy, A. Dosovitskiy, A. Fedorov, D. Kozlov, V. Mechinsky, R.W. Novotny, G. Tamulaitis, V. Vasiliev, H.-G. Zaunick, A.A. Vaitkevičius, Significant improvement of GAGG:Ce based scintillation detector performance with temperature decrease, Nucl. Instrum. Methods Phys. Res. Sect. A Accel. Spectrometers, Detect. Assoc. Equip. 871 (2017) 42–46.
[7] M.T. Lucchini, V. Babin, P. Bohacek, S. Gundacker, K. Kamada, M. Nikl, A. Petrosyan, A. Yoshikawa, E. Auffray, Effect of Mg^{2+} ions co-doping on timing performance and radiation tolerance of Cerium doped Gd3Al2Ga3O12 crystals, Nucl. Instrum. Methods Phys. Res. Sect. A Accel. Spectrometers, Detect. Assoc. Equip. 816 (2016) 176–183.
[8] E. Auffray, R. Augulis, A. Fedorov, G. Dosovitskiy, L. Grigorjeva, V. Gulbinas, M. Koschan, M. Lucchini, C. Melcher, S. Nargelas, G. Tamulaitis, A. Vaitkevičius, A. Zolotarjovs, M. Korzhik, Excitation transfer engineering in Ce-doped oxide crystalline scintillators by codoping with alkali-earth ions, Phys. Status Solidi Appl. Mater. Sci. 215 (2018) 1–10.
[9] V. Alenkov, O. Buzanov, A. Dosovitsky, G. Dosovitskiy, M. Korzhik, A. Fedorov, Garnet-type Single Crystal for Scintillation Detectors and its Production Technology, 2017, 2646407RU.
[10] M. Korzhik, et al., Compact and effective detector of the fast neutrons on a base of Ce doped Gd3Al2Ga3O12 scintillation crystal, IEEE Trans. 66 (2018) 536–540, https://doi.org/10.1109/TNS.2018.2888495.
[11] M.P. Taggart, M. Nakohostin, P.J. Sellin, Investigation into the potential of GAGG:Ce as a neutron detector, Nucl. Instrum. Methods 931 (2019) 121–126.
[12] P.L. Reeder, Neutron detection using GSO scintillator, Nucl. Instrum. Methods 340 (1994) 371–378.
[13] P.L. Reeder, Thin GSO scintillator for neutron detection, Nucl. Instrum. Methods 353 (1994) 134–136.
[14] J. Glodo, W.M. Higgins, E.V.D. van Loef, K.S. Shah, GdI3:Ce - a new gamma and neutron scintillator, in: IEEE Nuclear Science Symposium Conference Record, 2006.
[15] V. Alenkov, et al., Irradiation studies of a multi-doped Gd3Al2Ga3O12 scintillator, Nucl. Instrum. Methods 916 (2019) 226–229.
[16] Database of prompt gamma rays from slow neutron capture for elemental analysis, p.59.https://www.iaea.org/publications/7030/database-of-prompt-gamma-rays-from-slow-neutron-capture-for-elemental-analysis.
[17] J.L. Gräfe, F.E. McNeill, D.R. Chettle, S.H. Byun, Characteristic X ray emission in gadolinium following neutron capture as an improved method of in vivo measurement: a comparison between feasibility experiment and Monte–Carlo simulation, Nucl. Instrum. Methods Phys. Res. B 281 (2012) 21–25.
[18] http://sensl.com/downloads/ds/UM-ArrayTSV.pdf.
[19] State System for Ensuring the Uniformity of Measurements. Neutron Radiometers. Methods and Means of Verification. GOST 8.355-79 (in Russian).
[20] Portable Radiometric and Dosimetric Instruments. General Technical Requirements and Test Methods. GOST 28271-89 (in Russian).
[21] https://physics.nist.gov/PhysRefData/Xcom/html/xcom1.html.